



**UNIVERSITY OF LEEDS**

This is a repository copy of *An investigation of drug compact topography as relates to intrinsic dissolution rates determined by dissolution imaging*.

White Rose Research Online URL for this paper:

<https://eprints.whiterose.ac.uk/215967/>

Version: Accepted Version

---

**Article:**

Brown, B., Fazili, Z., Ward, A. et al. (4 more authors) (2021) An investigation of drug compact topography as relates to intrinsic dissolution rates determined by dissolution imaging. *Journal of Drug Delivery Science and Technology*, 61. 102143. ISSN 1773-2247

<https://doi.org/10.1016/j.jddst.2020.102143>

---

© 2021, Elsevier. This manuscript version is made available under the CC-BY-NC-ND 4.0 license <http://creativecommons.org/licenses/by-nc-nd/4.0/>. This is an author produced version of an article published in the *Journal of Drug Delivery Science and Technology*. Uploaded in accordance with the publisher's self-archiving policy.

**Reuse**

This article is distributed under the terms of the Creative Commons Attribution-NonCommercial-NoDerivs (CC BY-NC-ND) licence. This licence only allows you to download this work and share it with others as long as you credit the authors, but you can't change the article in any way or use it commercially. More information and the full terms of the licence here: <https://creativecommons.org/licenses/>

**Takedown**

If you consider content in White Rose Research Online to be in breach of UK law, please notify us by emailing [eprints@whiterose.ac.uk](mailto:eprints@whiterose.ac.uk) including the URL of the record and the reason for the withdrawal request.



[eprints@whiterose.ac.uk](mailto:eprints@whiterose.ac.uk)  
<https://eprints.whiterose.ac.uk/>



## Research paper

# An investigation of drug compact topography as relates to intrinsic dissolution rates determined by dissolution imaging

Benedict Brown<sup>a,b</sup>, Zayeeem Fazili<sup>a,b</sup>, Adam Ward<sup>a</sup>, Karl Walton<sup>b</sup>, Liam Blunt<sup>b</sup>, Jesper Østergaard<sup>c</sup>, Kofi Asare-Addo<sup>a,\*</sup>

<sup>a</sup> Department of Pharmacy, University of Huddersfield, Huddersfield, HD1 3DH, UK

<sup>b</sup> EPSRC Future Metrology Hub, University of Huddersfield, Huddersfield, HD1 3DH, UK

<sup>c</sup> Department of Pharmacy, University of Copenhagen, Universitetsparken 2, DK-2100, Copenhagen, Denmark



## ARTICLE INFO

## Keywords:

Ketoprofen  
Paracetamol  
Ibuprofen  
Intrinsic dissolution rate  
UV-Imaging  
Focus variation microscopy  
Dissolution imaging

## ABSTRACT

The purpose of this study was to characterize compact surfaces (surface roughness) and study its potential importance to the intrinsic dissolution rate (IDR) as determined by dissolution imaging. To this end, the effect of varying compaction pressures and the use of two stainless-steel surfaces with different textures/roughness on the intrinsic dissolution were investigated. Ketoprofen (KET), paracetamol (PAR) and ibuprofen (IBU) were compacted and a focus variation microscope used to determine the surface topology of the compacts. IDR determination was conducted using a surface dissolution imaging apparatus with the flow-through set up in phosphate buffer at pH 7.2 and at 37 °C. The results indicated a general decrease in the surface area of the drug compacts with an increase in compaction force (p values < 0.05 for IBU and PAR but not KET). This change in surface area was measured using the *S<sub>dr</sub>* parameter, which can be defined as the developed interfacial area. The smoother stainless-steel plate insert produced significantly smoother compacts for KET (*S<sub>dr</sub>* decreased from 0.30% to 0.07%). However, PAR and IBU compacts showed an increase in their *S<sub>dr</sub>* values from 3.94% to 17.90% and from 0.60% to 0.83%, respectively, suggesting the changes in surface properties to be drug specific relating to poor compaction properties and elasticity. The dissolution studies suggested that low compaction forces were not suitable for PAR. Overall changes in the surface topology did not have a significant effect on the obtained IDR values.

## 1. Introduction

The need to reduce the cost and time from the identification of a new chemical entity (NCE) to its eventual dosage form is of great importance in the pharmaceutical industry. The Biopharmaceutical classification system (BCS) is used to classify compounds [1,2] according to their solubilities and permeation behaviour. For some compounds, solubility alone has been shown to be a poor predictor of in-vivo drug performance [3,4]. Thus, to guide formulation development, dissolution (rate) is frequently determined [5]. Traditional compendial dissolution testing instrumentation requires a relatively large amount of compound. As the amount of compound available at early stage development is limited, these compendial dissolution methods are often not suitable [6,7].

In the context of the BCS solubility classification, highly soluble APIs

have been suggested to possess intrinsic dissolution rates above 0.1 mg min<sup>-1</sup> cm<sup>-2</sup>, whereas rates below this limit would often be attributed to APIs with a low BCS solubility classification [8]. Albeit a seemingly simple parameter, the determination of intrinsic dissolution rates remains challenging [9,10]. Intrinsic dissolution rate (IDR), the rate of dissolution adjusted for the surface area of a compound (e.g., µg/min/cm<sup>2</sup>), is measured while controlling the surface area available for dissolution and applying sink conditions [5,9]. Factors, such as the hydrodynamics, can affect IDR measurements as IDR is not an absolute drug property [11]. Besides from experimental setup variations such as hydrodynamics, variation in drug compacts surface area may also cause increases in variation of drug IDR; particularly when compact homogeneity is a concern [12]. In IDR determination utilizing miniaturized, sample sparing set-ups, the control of compact surface properties

**Abbreviations:** NCE, new chemical entity; API, active pharmaceutical ingredient; BCS, biopharmaceutical classification system; SDI, surface dissolution imaging; IDR, Intrinsic dissolution rate; KET, ketoprofen; PAR, paracetamol; IBU, Ibuprofen; XRPD, X-ray powder diffraction.

\* Corresponding author.

E-mail address: [k.asare-addo@hud.ac.uk](mailto:k.asare-addo@hud.ac.uk) (K. Asare-Addo).

<https://doi.org/10.1016/j.jddst.2020.102143>

Received 19 August 2020; Received in revised form 30 September 2020; Accepted 3 October 2020

Available online 10 October 2020

1773-2247/© 2020 Elsevier B.V. All rights reserved.

becomes even more important. Loosely attached API particles on the surface of compacts may give rise to erroneous data, for this reason, in some studies, data from the beginning of the experiment are excluded [7,13,14]. The Miniaturized INtrinsic DISSolution screening (MINDISS) assay [13], the  $\mu$ DISS Profiler [15,16], the Partially Automated Solubility Screening (PASS) assay [17], the miniaturized assay for solubility and residual solid screening (SORESOS) [18], the SiriusT3 and inForm are compound sparing techniques developed for IDR determination [5].

Surface Dissolution Imaging (SDI) instrumentation with Actipix™ Technology (Sirius Analytical now Pion) offers a UV-Vis imaging platform and a compound sparing approach that has been used for determining IDRs [7,14,19–25]. This flow-through based technique typically requires 5–10 mg of API with an experimental run time of 20–30 min for IDR determination. UV imaging has also been useful in other applications, such as biorelevant characterisation of salts, solid dispersions, transdermal patches, and hydrogels [26–36]. Alongside, the potential of the technique in relation to quality control assessment has been suggested [20,34,37].

The use of complementary imaging to inspect drug compacts prior to IDR determination is not a new concept. Both qualitative and quantitative approaches have been used previously. Madelung et al. utilised SEM and SEM-EDX to detect surface inhomogeneities on the API discs potentially affecting dissolution behaviour [38]. Alsenz et al. used optical microscopy to inspect compacts prior to IDR determination [11]. Hiew et al. also used optical microscopy, but however gained quantitative data with the attachment of a Raman spectrometer. This combination was used to analyse drug content of drug-exciipient compacts prior to IDR determination with an Actipix SDI 300 [39]. Focus variation microscopy has also been employed to suggest that rough drug compact surfaces, may increase the variation of IDR measurements [14,34,35].

The primary aim of this research was to study the importance of drug compact preparation and properties on the consistency/variability of intrinsic dissolution rate measurements. This aim was explored by firstly varying the compression pressure and secondly, varying the surface which the drug powder was compacted against by manufacturing a relatively “smoother” plate insert. Four different compaction forces were investigated to determine their effect on the IDR. KET and IBU were used as model BCS class II compounds (poorly soluble, highly permeable). IBU has poor compaction properties and the propensity to stick to tablet presses [40]. PAR is used as a model BCS class III compound (highly soluble, poorly permeable) and has reported poor compaction properties [41,42]. A focus variation instrument (Alicona Imaging GmbH, Graz, Austria), which is widely used in micro-precision manufacturing (typically for quality assurance) was used to acquire topographic surface height data in profile (2D) and area (3D) formats along with true colour surface images [43–45]. In this study, focus variation microscopy was also utilised to gain insights regarding the surface properties of the drug compacts.

## 2. Materials and methods

### 2.1. Materials

Ketoprofen (KET), Paracetamol (PAR) and Ibuprofen (IBU) were purchased from TCI chemicals (Oxford, UK). Monobasic potassium phosphate and sodium hydroxide were purchased from Sigma Aldrich, UK, and used in the preparation of 0.2 M phosphate buffer at pH 7.2 according to the USP 2019 method [46] for the dissolution experiments.

### 2.2. Methodology

#### 2.2.1. Preparation of compacts for surface analysis and IDR determinations

Compacts were made using the compact preparation kit (Fig. 1) on a computer-controlled M500-50CT instrument with compression plates (Testometric Co. Ltd., UK) A pre-set maximum pressure was set and the compacts for both KET, PAR, and IBU compressed with the displacement

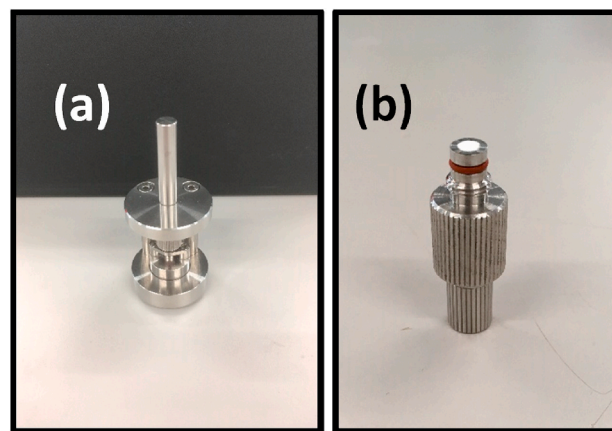


Fig. 1. (a) Compact preparation kit, (b) sample compact holder for IDR determination.

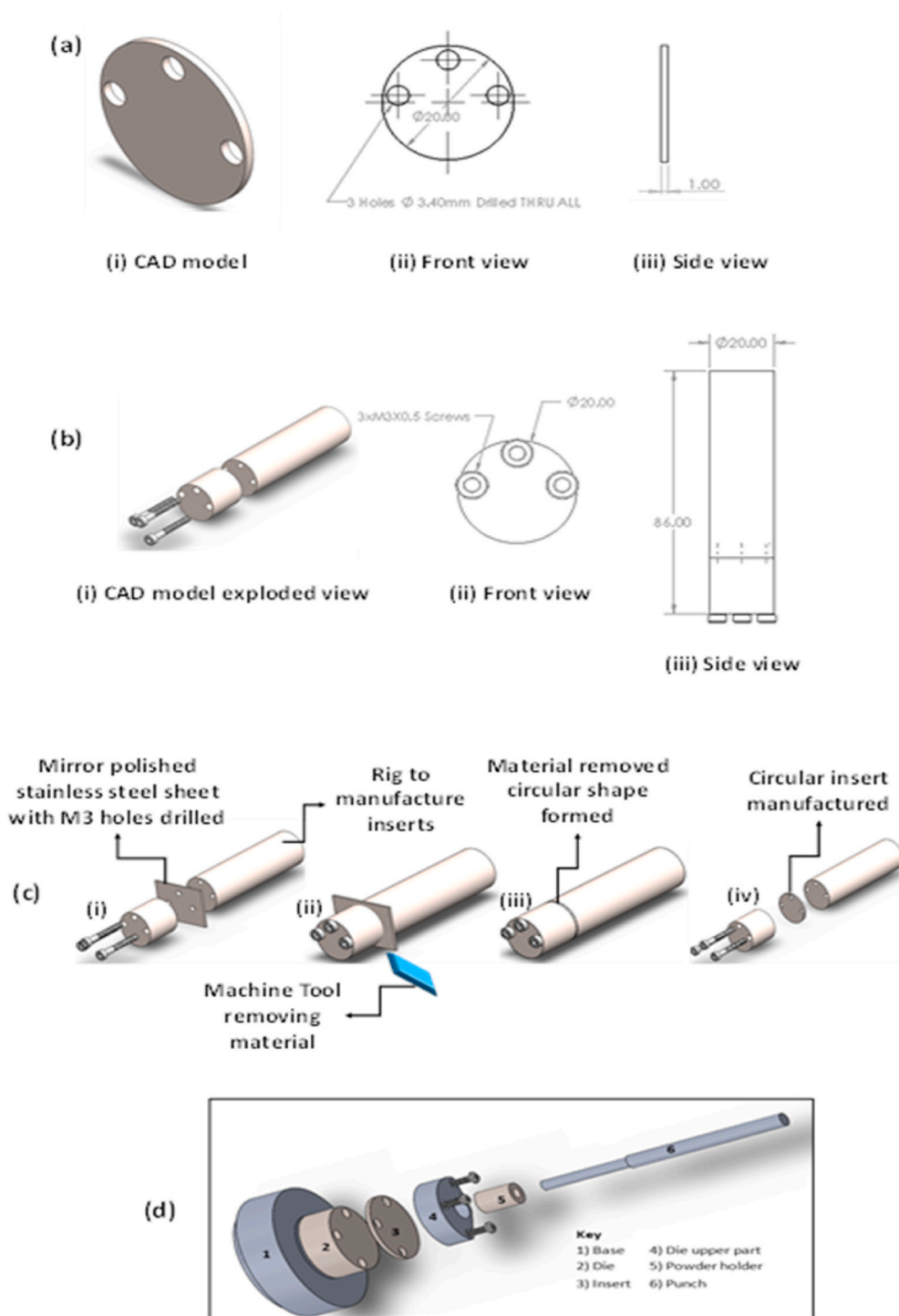
accurately measured using a short-travel extensometer at a set speed of  $1 \text{ mm min}^{-1}$ . KET, PAR and IBU were compacted at 0.25 kN, 0.49 kN, 0.74 kN and 0.98 kN. The target weight for all compacts was 15 mg with a variation allowance of  $\pm 0.2 \text{ mg}$ . One way ANOVA testing ( $\alpha = 0.05$ ) was used to compare the effects of compaction pressure on both IDR and *Sdr* for the four compaction pressures with post hoc Tukey's testing applied if significance was reached. Two tailed t-tests ( $\alpha = 0.05$ ) were used to compare the effects of the introduction of the smoother plate insert on IDR and *Sdr* for compacts made at a 0.98 kN compression force.

#### 2.2.2. Tooling effects on the compacts surface analysis

To determine the effect of the tooling on the surface of the compacts and its potential effect on the IDRs, a polished stainless-steel plate was manufactured. SolidWorks® (2018) CAD software was used to design the insert and the rig used for manufacturing the insert. The 3D CAD model and the 2D schematic of the insert and the rig are depicted in Fig. 2a and b. The rig in Fig. 2b was manufactured from a 316-grade stainless-steel bar. The steel bar was machined on a CNC lathe (Harrison L4 Engineering lathe), and three  $M3 \times 0.5$  holes 20 mm deep were drilled into the rig. The manufactured rig was then chuck mounted and a  $50 \text{ mm} \times 50 \text{ mm}$  (H  $\times$  L) mirror-polished stainless-steel grade 316 sheet of 1 mm thickness was inserted into the rig and excess material was removed to create a circular insert. Before the sheet was inserted into the rig, three holes of diameter 3.4 mm were drilled into the sheet such that the holes in the rig and sheet were aligned (Fig. 2c). After the insert was manufactured, it was assembled to the compact forming tooling (Fig. 2d). Upon manufacturing, the plate was inserted as depicted (Fig. 2d) and compacts of KET, PAR, and IBU were made as described in section 2.2.1.

#### 2.2.3. Surface analysis of tooling and compacts

The surface topography of the original press surface, the developed plate and compacts (3 mm) was analysed using focus variation microscopy (Alicona Infinite Focus microscope, Graz, Austria). Magnifications of 10x and 20x were selected based on previous work by Ward et al. [12]. The data from the microscope were processed using the program SurfStand [47] providing 3D surface parameters used to characterize the surface topography. Focus variation microscopy relies on different objectives to provide the required sensitivity to resolve the surface. The 20x magnification was selected to achieve the desired vertical resolution of  $0.05 \mu\text{m}$  which was within the recommended microscope operating limits [48]. Using the 20x magnification, 16 images of each compact were taken and automatically stitched together to resolve the whole surface with the required detail. Fig. 3 shows the process from taking the measurements to data processing. The limitation of this technique to transition between surface textures is described in literature [48]. For



this reason, the edges of each compact were cropped out as shown in Fig. 3. This ensured that erroneous data was not measured from the incidental measurement of the metal rim of the compact. Additionally, images were also cut to the same size to ensure uniformity in data treatment and to allow comparison of the nature of the drug surfaces.

The *Sdr* parameter, which is the developed interfacial (surface) area ratio (equation (1)) allowed the influence of the different compressions on the surface topology of the compacts to be evaluated. *Sdr* is defined as the surface area gain of the textured sample surfaces compared to that of its cross-sectional area. By doing this comparison of textured surface area gain, the parameter *Sdr* is always expressed as a percentage where the cross-sectional area of a surface is zero percent and any texture to

this same surface will increase the *Sdr* percentage, relative to that of the cross-sectional area. This allows for the surface gain (surface area) to be calculated meaning that differences between the compacts made from the original press surface and the developed plate can be ascertained. The same compacts used for the *Sdr* measurements were used for IDR determinations. Along with the *Sdr* data, 23 other surface parameters were also generated for each compact surface. Although, some of these other surface parameters were shown to be of some use in the analysis of drug compacts [49], this study focused solely on the *Sdr* parameter with the aim of showing a direct relationship between surface gain and IDR determination performance.

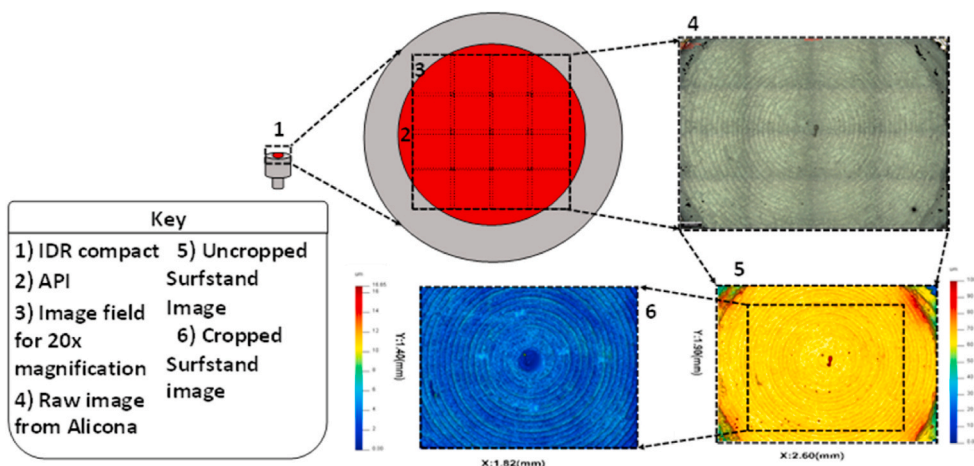


Fig. 3. Schematic representation of the measurement zone for the 20x magnification used from which the developed interfacial (surface) area ratio (*Sdr*) was determined.

$$Sdr = \frac{(Texture\ Surface\ Area) - (Cross\ Sectional\ Area)}{Cross\ Sectional\ Area} \times 100 \quad (1)$$

#### 2.2.4. Dissolution imaging

The SDI2 compact flow cell (Fig. 4a) was used for the IDR determinations. Each dissolution experiment lasted 21 min (including 1 min period where a higher flow rate of 5 mL/min was applied to fill the compact flow cell). This was implemented to flush away loose particles on the surface. A flow rate of 2.0 mL/min was applied for the following 20 min. The experiments were conducted in phosphate buffer (pH 7.2) at 37 °C. Dissolution imaging was conducted at the wavelengths 255 nm (UV) and 520 nm (Vis). All experiments were conducted 5 times (n = 5).

Analysis of the dissolution images was performed using the SDI2 software (Pion Inc., version 3.0.22). The molar extinction coefficients for the drugs were experimentally determined over seven concentration levels (KET: 2 µg/mL - 18 µg/mL, PAR: 10 µg/mL - 80 µg/mL and IBU: 25 µg/mL - 500 µg/mL) in the phosphate buffer (pH 7.2). Calibration curves were derived from two stocks solutions and conducted in triplicate and had *r*<sup>2</sup> values ranging from 0.9919 to 0.9966 (all calibration

curves were within the linear range). A 1 cm by 1 cm box was set to collect absorbance values and placed in the middle of the cell (red arrow on Fig. 4b). Absorbance data for the calibration curve were collected at 30 s intervals over the last 5 min of each 10 min run of the standards. Intrinsic dissolution rates were calculated by incorporating the molar extinction coefficient (MEC) of each drug into the provided software (Pion Inc., version 3.0.22).

#### 2.2.5. X-ray powder diffraction (XRPD)

The XRPD patterns were determined for the bulk powders of KET, IBU and PAR. XRPD patterns were also determined after the compaction process (powder was removed from the compact disc and analysed) and after the 21 min long IDR experiment (powder was removed after drying in an oven at 40 °C for an hour and analysed) for compacts made at a compaction force of 0.98 kN. This allowed for the influence of the compression and dissolution process on the solid-state properties of the compacts to be assessed. All compacts were scanned in Bragg-Brentano geometry, over a scattering (Bragg, 2θ) angle range from 5 to 100°, in 0.02° steps at 1.5° min<sup>-1</sup> using a D2 Phaser diffractometer (Bruker AXS

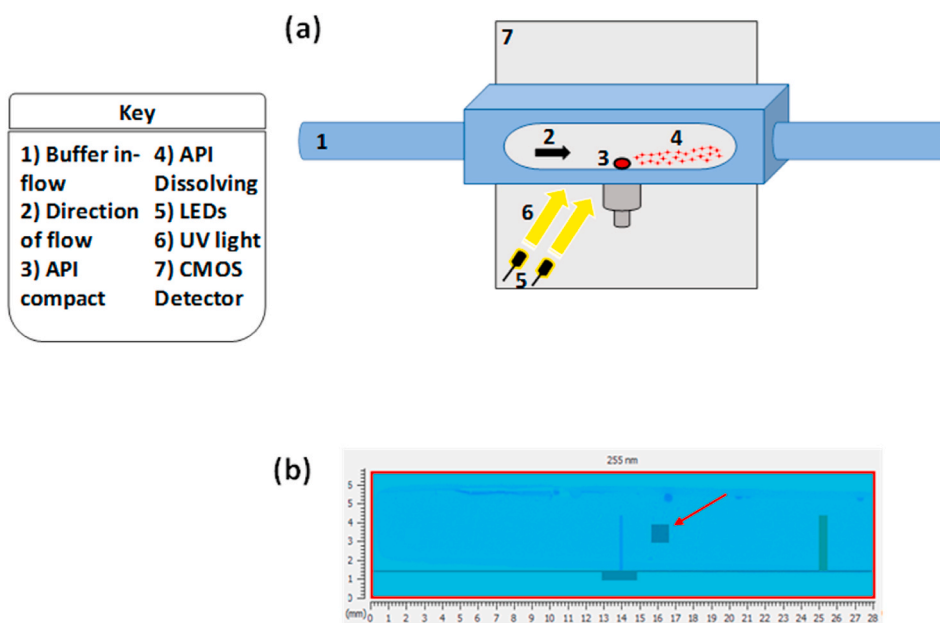


Fig. 4. (a) Schematic representation of a compact flow-through cell for the SDI2 system for IDR determinations (b) 1 cm × 1 cm box used in the data collection for the calibration of either KET, PAR or IBU for molar extinction coefficient determinations.

GmbH, Karlsruhe, Germany) [50]. Microsoft Excel was used to analyse the collected XRPD patterns.

### 3. Results and DISCUSSION

#### 3.1. Impact of tooling on the surface topography of the compacts

The quality of compacts and their surfaces may affect drug dissolution behaviour. Andersson et al. reported that the quality of the disc during disc dissolution affected the variability of IDR values using the  $\mu$ DISS [9]. The focus variation instrument provides quantitative data that allows for the topology of surfaces to be investigated. Fig. 5a and b depict the images of the surfaces of the original press surface and the manufactured steel plate insert, respectively.

The images highlight the differences with respect to the roughness of the surfaces, which may affect the surfaces of the compacts produced. The manufactured plate insert had a significantly lower *Sdr* (8.6%) as compared to that of the original press surface (19.9%). The IBU compacts (from the original press surface) show visually that an increase in the compression force of the compacts brought about a decrease in the compact surface roughness (Fig. 5c). This was also evident from Table 1, where generally, the higher the compression force, the lower the *Sdr* value of the compact. One way-ANOVA testing showed that the changes in compaction force had a significant effect on the *Sdr* with PAR and IBU ( $p < 0.05$ ) but not for KET ( $p > 0.05$ ). However, a *Tukey's* post hoc test of PAR failed to identify any trend in the *Sdr* data indicating that there was not a strong correlation between compaction force and the surface roughness of the PAR compacts. These findings may be due to the elastic nature of PAR [40,41]. Post hoc *Tukey's* testing with IBU showed that higher compaction forces resulted in a lower *Sdr*. In respect to *Sdr* no distinction between 0.98 kN and 0.74 kN could be made. However, statistical testing showed that the 0.98 kN and 0.74 kN compaction forces resulted in a lower *Sdr* when compared to 0.49 kN and that all compaction forces were given a lower *Sdr* when compared to the 0.25 kN.

**Table 1**

Developed interfacial (surface) area ratio (*Sdr*) for KET, PAR and IBU 3 mm compacts from the different compaction forces and the manufactured plate insert (at 0.98 kN plate). All experiments were conducted 5 times ( $n = 5$ ) and reported with their standard deviations.

Compact	Ketoprofen (KET)	Paracetamol (PAR)	Ibuprofen (IBU)
	<i>Sdr</i> (%)	<i>Sdr</i> (%)	<i>Sdr</i> (%)
0.25 kN	3.3 ± 3.6	5.0 ± 1.1	8.3 ± 1.1
0.49 kN	0.6 ± 0.4	7.6 ± 2.1	3.2 ± 0.6
0.74 kN	0.3 ± 0.1	7.2 ± 2.9	1.4 ± 0.2
0.98 kN	0.3 ± 0.0	3.9 ± 1.6	0.6 ± 0.2
0.98 kN plate	0.1 ± 0.0	17.9 ± 12.7	0.8 ± 0.5

Fig. 6 depicts the images of compact surfaces obtained from the compaction force at 0.98 kN for the original press surface and the manufactured plate insert using the focus variation microscope. With the introduction of the plate insert, KET showed a reduction in *Sdr* from 0.3% (original press surface) to 0.1% (manufactured plate insert) (Fig. 6a and Table 1). This was very close to a theoretical flat plane of 0%. These surfaces were shown to be statistically different ( $p < 0.05$ ).

Using the compaction pressure of 0.98 kN, the manufactured plate insert caused an increase in the *Sdr* values for PAR and IBU (Fig. 6b and c, Table 1). For PAR especially, there was a large increase in the mean *Sdr* value (3.9%) to (17.9%). These differences in the *Sdr* for PAR and IBU were however not statistically significant. This may be due to the higher standard deviations experienced by the PAR and IBU compacts thereby indicating a decrease in repeatability. This is evident in the individual images ( $n = 5$  images) obtained from the focus variation instrument (images not included).

XRPD (supplementary material) showed that the PAR used was form I. This form tends to have poor compaction properties resulting from a crystal structure of corrugated hydrogen-bonded layers, which lack the ability to stack flat [37,38]. It would seem, in the case of PAR and IBU, that the ring like pattern from the original press surface may be

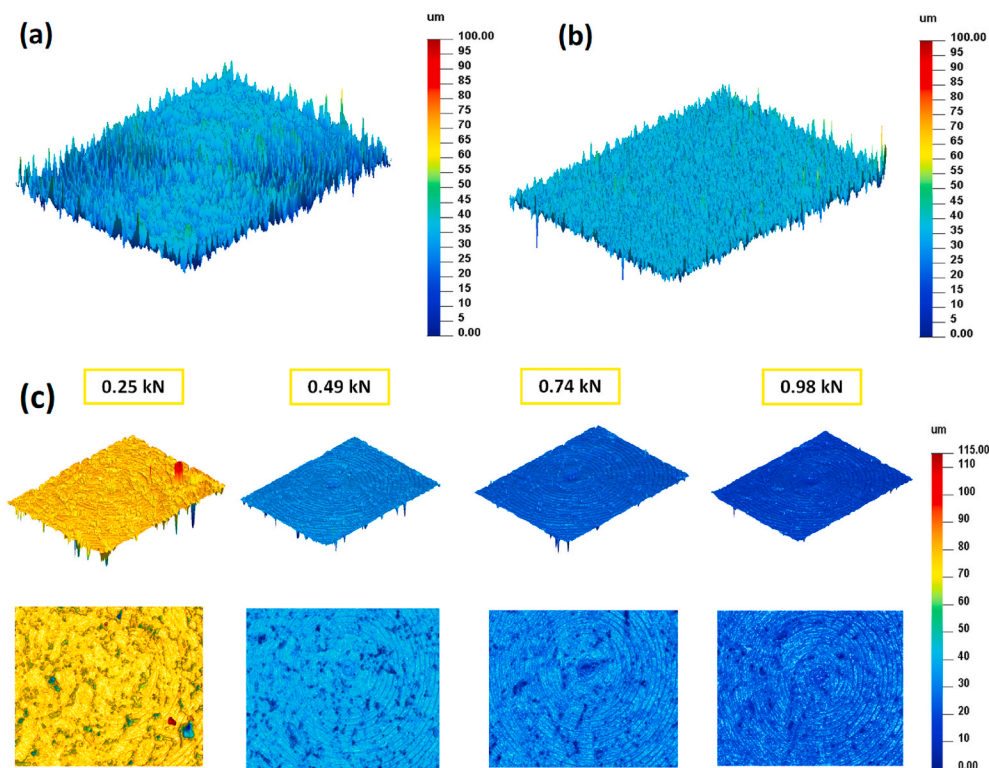


**Fig. 5.** 3D images of the roughness of the original (a), and the manufactured plate insert surfaces (b), both used in the production compacts for IDR determinations. 3D images of the surfaces of IBU compacts at varying compressions of forces using the original press surface (c).

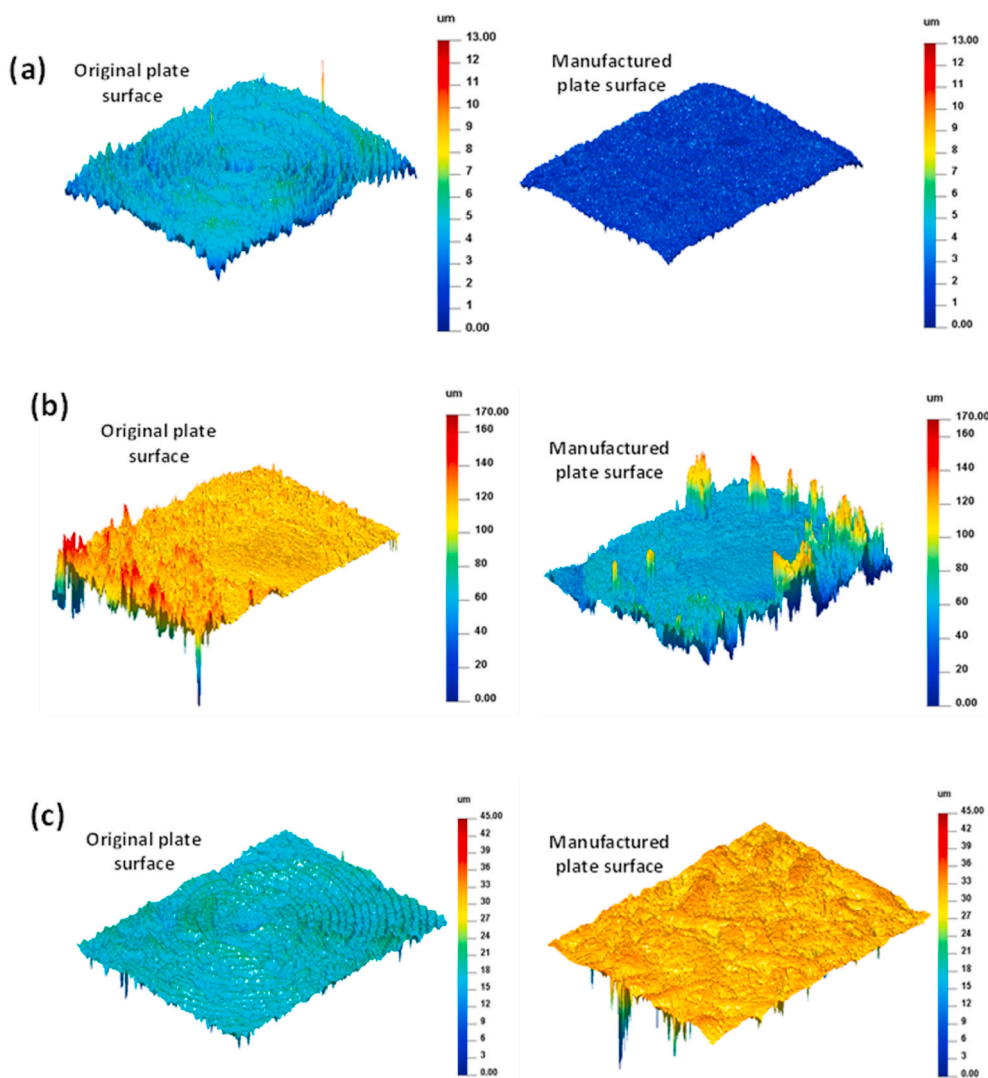


Fig. 6. 3D images of the surface roughness from the focus variation instrument for (a) KET, (b) PAR (c) IBU compacts at 0.98 kN using the original press surface and the manufactured plate insert also at 0.98 kN.

preferable, as the added texture provides a surface that is less prone to sticking. The relatively smoother inserted plate seems to be of no or very limited benefit to such APIs and therefore care and consideration should be given to the nature of API during the compact preparation process.

### 3.2. Intrinsic dissolution rate determinations

Figs. 7a, 8a and 9a depict the UV images for the IDR determinations of KET, PAR and IBU respectively. The images for each compaction force were seen to be very similar. This correlated well to similar IDR values for each of the APIs over the course of the experiments. In the dissolution studies (at every test condition), the IDR of the drug substances had reached a plateau by 5 min. The blue, red and yellow inserts in Figs. 7–9c for KET, PAR and IBU, respectively, showed increased variability prior to the 5 min mark. This high IDR variability from the 0–5 min mark may have been attributed to the dissolution of residual/loose drug particles on the surface of the compacts. The initial high IDR variability phase has also been the region in which fractal-like dissolution as described by Niderquell and Kuentz has been observed [20]. This phenomenon may be caused by differences in crystal morphology or the particle size of drug on the compact surface [20]. This was particularly prominent for KET (Fig. 7b and c). IDR values for both PAR and IBU reached a plateau

quicker as seen in Fig. 8b, c, and Fig. 9b, c respectively.

Although most images for all IDR determinations looked similar, differences can be found with the PAR 0.25 kN after the 15 min time point. Large amounts of PAR were seen in the dissolution stream in the image field. This inflated the average IDR value from  $339 \mu\text{g}/\text{min}/\text{cm}^2$  (pre 15 min) to  $1814 \mu\text{g}/\text{min}/\text{cm}^2$  (post 15 min). This was also visualised in Fig. 8b (indicated by the red arrow) where the increase in the absorbance lead to a significant increase in the IDR value of PAR. Upon further inspection of the images and the compact post dissolution, it appeared a complete breakdown of the compact had occurred. This suggested a compaction force of 0.25 kN was too low for PAR. Additionally a “wave” (red arrow on Fig. 8a) was also seen in the UV image for the 0.98 kN compact (with the manufactured plate insert). This wave formation may have been PAR particulates dissolving faster into the dissolution stream from the compact.

Table 2 depicts the average IDR values of the API's post 5 min. The data did not exhibit a trend in IDR values ( $p > 0.05$ ) or their standard deviations with respect to compaction force changes. This was consistent with work by Alsenz et al. where a range of compaction forces from 0.07 kN to 0.2 kN used to compact 4 mg micro discs of KET for miniaturized IDR determination did not demonstrate any significant effects on the IDR [13]. Löbmann et al. did not show any significant correlation between IDR and compaction pressure using crystalline indomethacin,

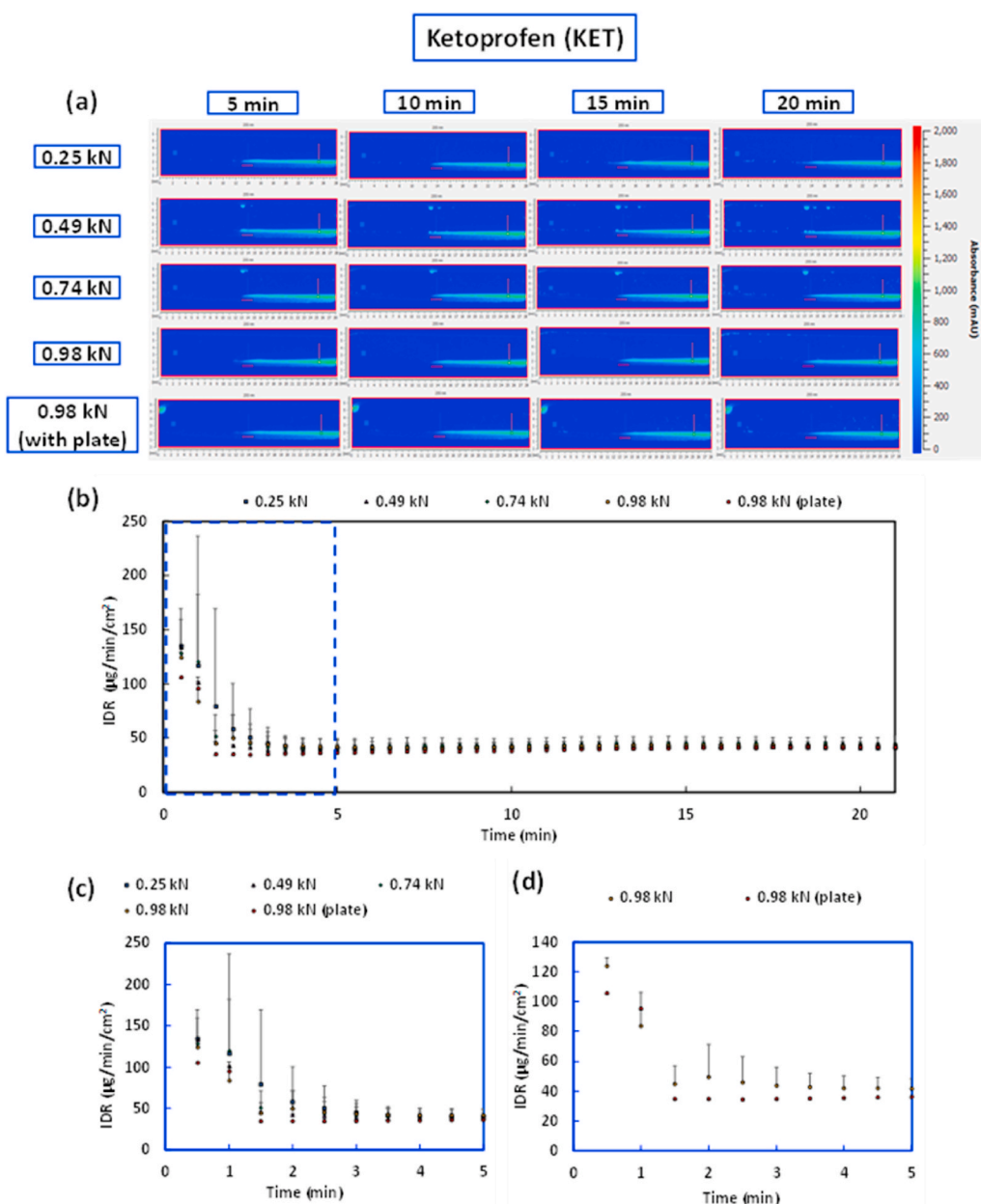


**Fig. 7.** (a) Surface dissolution imaging of KET at 0.25, 0.49, 0.74, 0.98 and 0.98 kN (with manufactured plate) at 5, 10, 15 and 20 min time points. (b) IDR as a function of time for of KET at 0.25, 0.49, 0.74, 0.98 and 0.98 kN (with manufactured plate). Blue insert in Fig. 7b is to elaborate this point hence why IDR was reported after the 5 min mark only. The zoom-in of the blue insert is depicted as Fig. 7c for clarity. Fig. 8d compares the compacts at 0.98 kN with and without the plate insert to show the significant reduction in variability as a result. (For interpretation of the references to colour in this figure legend, the reader is referred to the Web version of this article.)

however this was not the case for the amorphous form [25]. This indicates that any correlation between IDR performance and compaction force may be form dependent.

The introduction of the manufactured plate had little effect on the IDR determinations. The recorded changes in the IDR values were not statistically significant. This suggests that the use of the manufactured plate insert did not improve IDR determination or that the inferior surface properties actually spilled over to variation with respect to dissolution behaviour. This is also evident on Fig. 6c where the manufactured plate insert increased the surface roughness of the IBU compacts thereby increasing the surface heterogeneity.

For all test conditions, the relative standard deviation (expressed here as a percentage for comparison purposes) of the IDR value varied between 1 and 13% (average 7%) for KET, 5–96% (average 25%) for PAR and 14–57% (average 33%) for IBU. The apparent larger variation in the PAR IDR determination is largely skewed by the inflated IDR determination for the 0.25 kN experiments. Similar levels of variation have been reported using the Sirius SDI dissolution imaging system, a predecessor of the instrument applied in the current study [10], and the

$\mu$ DISS Profiler™ [9]. Etherson et al. reported in an inter-laboratory small-scale dissolution study that the relative standard deviation (expressed as a percentage) of IDR values varied from 33 to 130% using 6 compounds ( $n = 6$ ), and FaSSIF and blank FaSSIF as the dissolution media across seven sites [10]. For IBU, there was a large variation in the absolute measured IDR values from the two generations of the SDI equipment. Etherson et al. using the first generation recorded an IDR for IBU of  $66 \mu\text{g}/\text{min}/\text{cm}^2$  ( $n = 6$ ), using blank FaSSIF version 1 [46], whereas this study using the second generation reports an IBU IDR of  $320 \mu\text{g}/\text{min}/\text{cm}^2$  using phosphate buffer, pH 7.2, as the dissolution media. This vast difference in absolute IDR values between the first generation (SDI) and second generation (SDI2), may be attributed to the different media used, however it is also highly likely that experimental set-up and data processing had an impact. Using the  $\mu$ DISS Profiler™, Andersson et al. also found IDR measurements with similar levels of relative standard deviation (35–127%, expressed as a percentage for comparison purposes), with 6 compounds ( $n = 3$ ), using FaSSIF and phosphate buffer pH 6.5 as the dissolution media. This would indicate that each of these small-scale IDR determination methods give similar



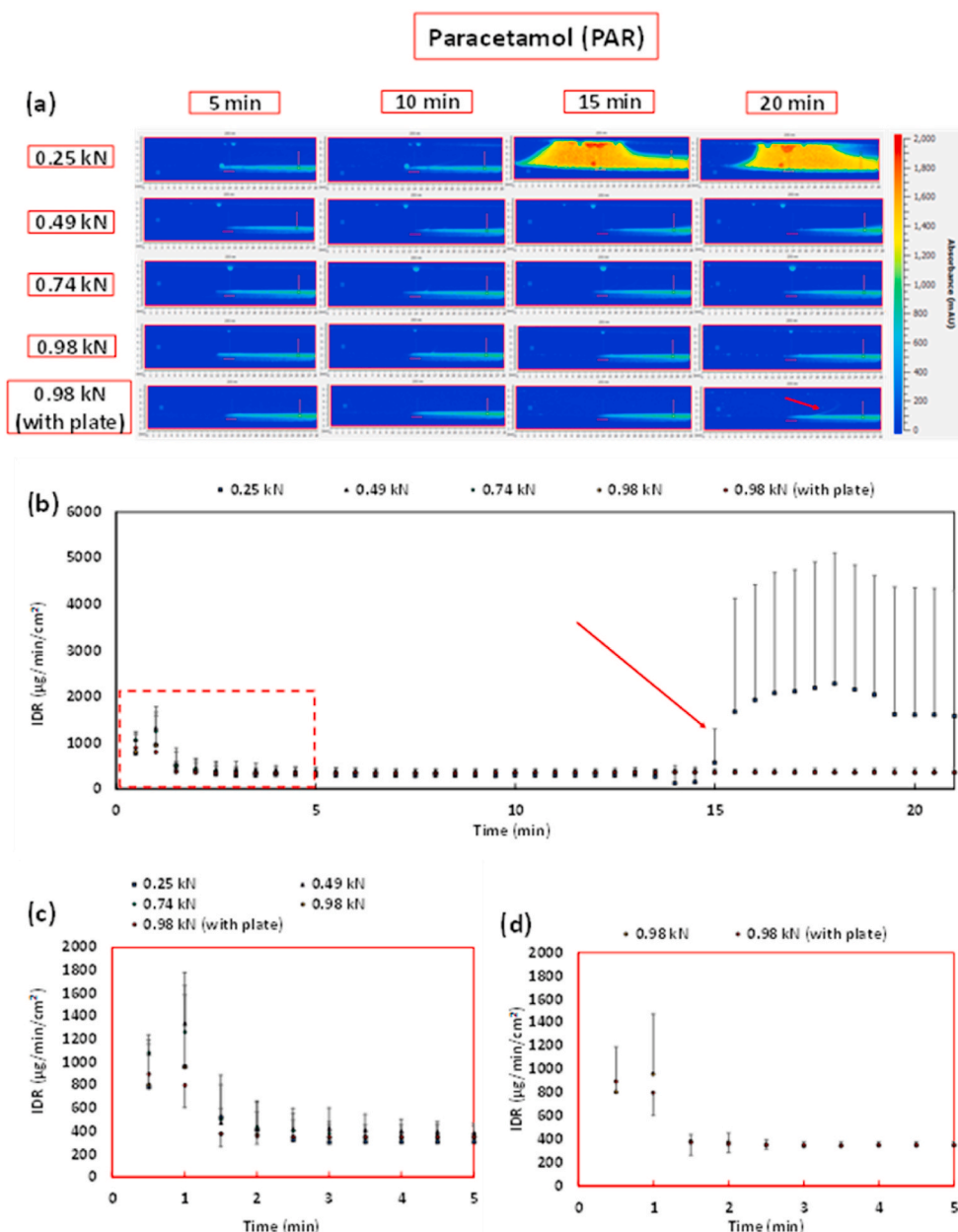


**Fig. 8.** (a) Surface dissolution imaging of PAR at 0.25, 0.49, 0.74, 0.98 and 0.98 kN (with manufactured plate) at 5, 10, 15 and 20 min time points. (b) IDR as a function of time for PAR at 0.25, 0.49, 0.74, 0.98 and 0.98 kN (with manufactured plate). The red insert in Fig. 8b is to elaborate this point hence why IDR was reported after the 5 min mark only. The 0.25 kN compact failure is indicated by the red arrow. The zoom-in of the red insert is depicted as Fig. 8c for clarity. Fig. 8d compares the compacts at 0.98 kN with and without the plate insert to show the significant reduction in variability as a result. (For interpretation of the references to colour in this figure legend, the reader is referred to the Web version of this article.)

levels of variations.

XRPD (Supplementary Figs. S1–S3) showed that polymorphic changes did not occur during the compaction and IDR determination process. The XRPD distinctive peaks for KET, IBU and PAR are published elsewhere [14,37,40,51,52].

#### 4. Conclusion

This study demonstrated that surface characteristics of drug compacts can be successfully studied using focus variation microscopy. In general, higher compaction forces resulted in smoother compacts, although statistically significant differences were only reached for IBU, which suggests this relationship may be API dependent. For KET, the use of a relatively smooth manufactured plate insert produced a smoother compact as measured by a reduction in the  $Sdr$  value. The opposite was true for PAR and IBU compacts, which is most likely as a result of the poor compaction properties associated with these compounds. This suggests that the ability of a smooth compaction surface to produce a

smooth compact is also API dependent. Despite the differences in drug compact surfaces with changes in compaction force and changes in the compaction surface, statistical differences were not shown in the IDR measurements. The variation associated with measuring IDR using the SDI2, appears to be comparable to that of the other small-scale IDR determination methods. This study thus highlights the ability of the focus variation instrument to provide a quantitative way to analyse drug compacts surfaces prior to IDR determination.

#### CRediT authorship contribution statement

**Benedict Brown:** Data curation, Formal analysis, Methodology, Investigation, Writing - original draft, Writing - review & editing. **Zayeem Fazili:** Data curation, Formal analysis, Methodology, Investigation, Writing - original draft. **Adam Ward:** Data curation, Formal analysis, Methodology, Investigation. **Karl Walton:** Conceptualization, Supervision, Data curation. **Liam Blunt:** Conceptualization, Supervision. **Jesper Østergaard:** Methodology, Investigation, Writing - review

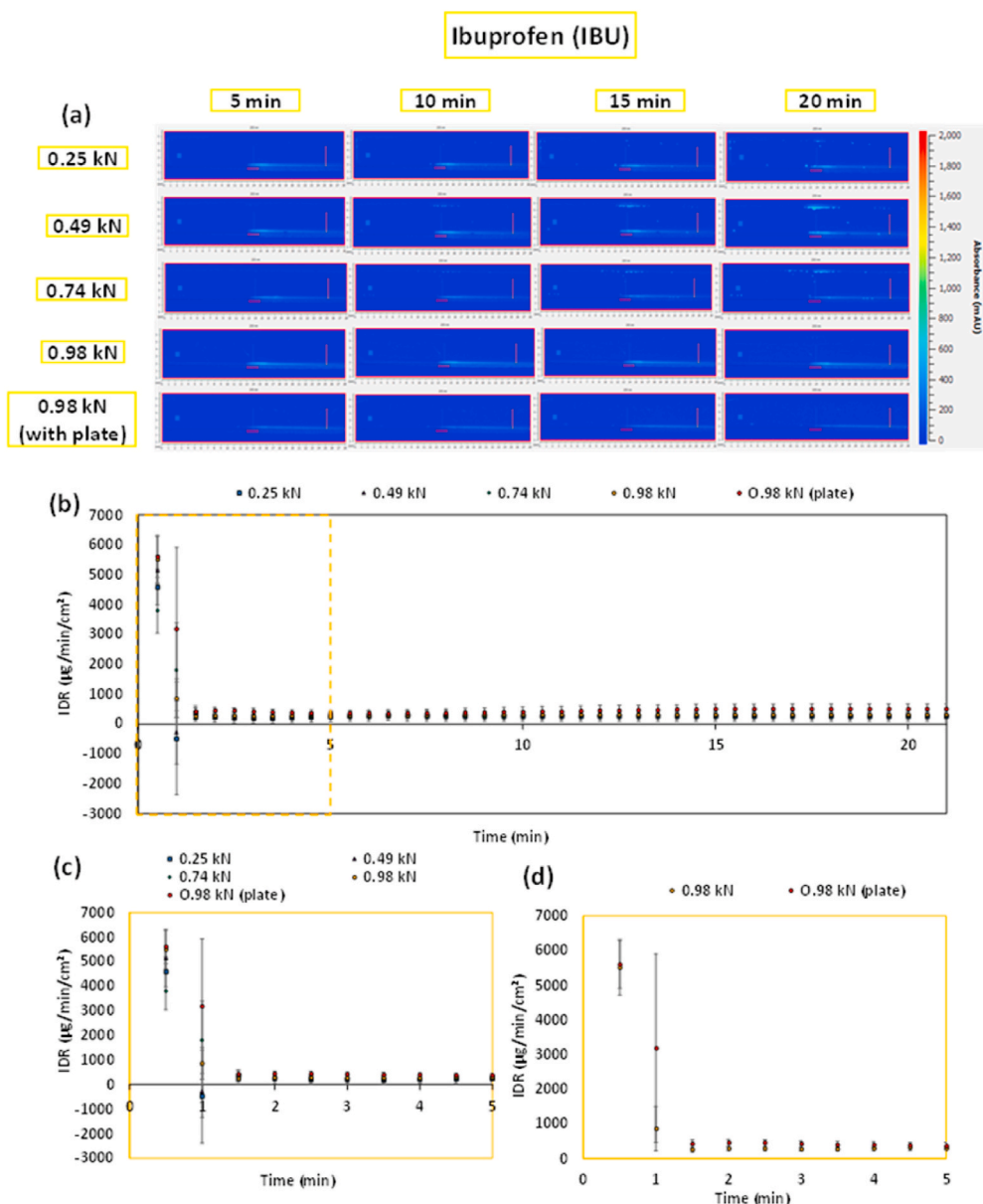


**Fig. 9.** (a) Surface dissolution imaging of IBU at 0.25, 0.49, 0.74, 0.98 and 0.98 kN (with manufactured plate) at 5, 10, 15 and 20 min time points. (b) IDR as a function of time for of IBU at 0.25, 0.49, 0.74, 0.98 and 0.98 kN (with manufactured plate). The zoom-in of the yellow insert is depicted as Fig. 9c for clarity. Fig. 9d compares the compacts at 0.98 kN with and without the plate insert to show the significant reduction in variability as a result. (For interpretation of the references to colour in this figure legend, the reader is referred to the Web version of this article.)

**Table 2**

Intrinsic dissolution rates (IDR) for KET, PAR and IBU 3 mm compacts from the different compaction forces and a manufactured plate insert. All experiments were conducted 5 times (n = 5) and reported with their standard deviations.

Compact	Ketoprofen (KET)	Paracetamol (PAR)	Ibuprofen (IBU)
	IDR ( $\mu\text{g}/\text{min}/\text{cm}^2$ )	IDR ( $\mu\text{g}/\text{min}/\text{cm}^2$ )	IDR ( $\mu\text{g}/\text{min}/\text{cm}^2$ )
0.25 kN	41 ± 3	1078 ± 1162	263 ± 168
0.49 kN	42 ± 1	375 ± 48	296 ± 79
0.74 kN	44 ± 7	355 ± 26	279 ± 62
0.98 kN	42 ± 4	364 ± 32	314 ± 49
0.98 kN plate	39 ± 3	357 ± 18	452 ± 146

& editing. **Kofi Asare-Addo:** Conceptualization, Supervision, Writing - original draft, Writing - review & editing.

**Declaration of competing interest**

The authors declare no conflict of interest.

**Acknowledgements**

The authors acknowledge the EPSRC DTP at the University of Huddersfield for financial support for Benedict Brown. The authors also acknowledge Becky Upton and Breeze Outwaite (formerly of Pion, UK), Hayley Watson and Karl Box of Pion, UK for their technical expertise on the use of the SDI2 instrument. The authors also thank Charlotte Ayres and Professor Jonathan Steed of the University of Durham for their assistance.

**Appendix A. Supplementary data**

Supplementary data to this article can be found online at <https://doi.org/10.1016/j.jddst.2020.102143>.

**References**

[1] G.L. Amidon, H. Lennernäs, V.P. Shah, J.R. Crison, A theoretical basis for a biopharmaceutic drug classification: the correlation of in vitro drug product dissolution and in vivo bioavailability, *Pharmaceut. Res.* 12 (3) (1995) 413–420.

- [2] N. Kanikkannan, Technologies to improve the solubility, dissolution and bioavailability of poorly soluble drugs, *J Anal Pharm Res* 7 (1) (2018), 00198.
- [3] C.A.S. Bergström, S.B.E. Andersson, J.H. Fagerberg, G. Ragnarsson, A. Lindahl, Is the full potential of the biopharmaceutics classification system reached? *Eur. J. Pharmaceut. Sci.* 57 (1) (2014) 224–231.
- [4] J.M. Butler, J.B. Dressman, The developability classification system: application of biopharmaceutics concepts to formulation development, *J. Pharmaceut. Sci.* 99 (12) (2010) 4940–4954.
- [5] C.A. Bergström, K. Box, R. Holm, W. Matthews, M. McAllister, A. Müllertz, A. Teleki, Biorelevant intrinsic dissolution profiling in early drug development: fundamental, methodological, and industrial aspects, *Eur. J. Pharm. Biopharm.* 139 (2019) 101–114, 6.
- [6] J. Mauder, J. Ballard, R. Brockson, S. De, V. Gray, D. Robinson, Intrinsic dissolution performance testing of the USP dissolution apparatus 2 (Rotating Paddle) Using modified salicylic acid calibrator tablets: proof of principle, *Dissolution Technol.* 10 (3) (2003) 6–15.
- [7] W.L. Hulse, J. Gray, R.T. Forbes, A discriminatory intrinsic dissolution study using UV area imaging analysis to gain additional insights into the dissolution behaviour of active pharmaceutical ingredients, *Int. J. Pharm.* 434 (1–2) (2012) 133–139.
- [8] L.X. Yu, A.S. Carlin, G.L. Amidon, A.S. Hussain, Feasibility studies of utilizing disk intrinsic dissolution rate to classify drugs, *Int. J. Pharm.* 270 (1) (2004) 221–227.
- [9] S.B. Andersson, C. Alvebratt, J. Bevernage, D. Bonneau, C. da Costa Mathews, R. Dattani, K. Edueng, Y. He, R. Holm, C. Madsen, Interlaboratory validation of small-scale solubility and dissolution measurements of poorly water-soluble drugs, *J. Pharmaceut. Sci.* 105 (9) (2016) 2864–2872.
- [10] K. Etherson, C. Dunn, W. Matthews, H. Pamelund, C. Barragat, N. Sanderson, T. Izumi, C. da Costa Mathews, G. Halbert, C. Wilson, M. McAllister, An interlaboratory investigation of intrinsic dissolution rate determination using surface dissolution, *Eur. J. Pharm. Biopharm.* 150 (2020) 24–32.
- [11] M. Kuentz, Analytical technologies for real-time drug dissolution and precipitation testing on a small scale, *J. Pharm. Pharmacol.* 67 (2) (2015) 143–159.
- [12] P. Macheras, A. Dokoumetzidis, On the heterogeneity of drug dissolution and release, *Pharmaceut. Res.* 17 (2) (2000) 108–112.
- [13] J. Alsenz, E. Haenel, A. Anedda, P. Du Castel, G. Cirelli, Miniaturized Intrinsic Dissolution Screening (MINDISS) assay for preformulation, *Eur. J. Pharmaceut. Sci.* 87 (2016) 3–13.
- [14] A. Ward, K. Walton, K. Box, J. Østergaard, L.J. Gillie, B.R. Conway, K. Asare-Addo, Variable-focus microscopy and UV surface dissolution imaging as complementary techniques in intrinsic dissolution rate determination, *Int. J. Pharm.* 530 (1–2) (2017) 139–144.
- [15] A. Avdeef, O. Tsinman, Miniaturized rotating disk intrinsic dissolution rate measurement: effects of buffer capacity in comparisons to traditional wood's apparatus, *Pharmaceut. Res.* 25 (11) (2008) 2613–2627.
- [16] C.M. Berger, O. Tsinman, D. Voloboy, D. Lipp, S. Stones, A. Avdeef, Technical note: miniaturized intrinsic dissolution rate (Mini-IDR™) measurement of griseofulvin and carbamazepine, *Dissolution Technol.* 14 (4) (2007) 39–41.
- [17] J.M.E. Alsenz, E. Haenel, Development of a partially automated solubility screening (PASS) assay for early drug development, *J. Pharmaceut. Sci.* 96 (7) (2007).
- [18] N. Wyttenbach, J. Alsenz, O. Grassmann, Miniaturized assay for solubility and residual solid screening (SORESOS) in early drug development, *Pharmaceut. Res.* 24 (5) (2007) 888–898.
- [19] C.M. Long, K. Tang, H. Chokshi, N. Fotaki, Surface dissolution UV imaging for investigation of dissolution of poorly soluble drugs and their amorphous formulation, *AAPS PharmSciTech* 20 (3) (2019) 1–12.
- [20] A. Niederquell, M. Kuentz, Biorelevant dissolution of poorly soluble weak acids studied by UV imaging reveals ranges of fractal-like kinetics, *Int. J. Pharm.* 463 (1) (2014) 38–49.
- [21] J.P. Boetker, M. Savolainen, V. Koradia, F. Tian, T. Rades, A. Müllertz, C. Cornett, J. Rantanen, J. Østergaard, Insights into the early dissolution events of amlodipine using UV imaging and Raman spectroscopy, *Mol. Pharm.* 8 (4) (2011) 1372–1380.
- [22] S. Gordon, K. Naelapää, J. Rantanen, A. Selen, A. Müllertz, J. Østergaard, Real-time dissolution behavior of furosemide in biorelevant media as determined by UV imaging, *Pharmaceut. Dev. Technol.* 18 (6) (2013) 1407–1416.
- [23] N. Qiao, K. Wang, W. Schlindwein, A. Davies, M. Li, In situ monitoring of carbamazepine–nicotinamide cocrystal intrinsic dissolution behaviour, *Eur. J. Pharm. Biopharm.* 83 (3) (2013) 415–426.
- [24] Y. Lu, M. Li, Simultaneous rapid determination of the solubility and diffusion coefficients of a poorly water-soluble drug based on a novel UV imaging system, *J. Pharmaceut. Sci.* 105 (1) (2016) 131–138.
- [25] K. Löbmann, K. Flouda, D. Qiu, T. Tzolakou, W. Wang, T. Rades, The influence of pressure on the intrinsic dissolution rate of amorphous indomethacin, *Pharmaceutics* 6 (3) (2014 Sep) 481–493.
- [26] S. Colombo, M. Brisander, J. Haglöf, P. Sjövall, P. Andersson, J. Østergaard, M. Malmsten, Medicinteknik, Matrix effects in nilotinib formulations with pH-responsive polymer produced by carbon dioxide-mediated precipitation, *Int. J. Pharm.* 494 (1) (2015) 205–217.
- [27] F. Ye, A. Yagmur, H. Jensen, S.W. Larsen, C. Larsen, J. Østergaard, Real-time UV imaging of drug diffusion and release from Pluronic F127 hydrogels, *Eur. J. Pharmaceut. Sci.* 43 (4) (2011) 236–243.
- [28] J. Østergaard, E. Meng-Lund, S.W. Larsen, C. Larsen, K. Petersson, J. Lenke, H. Jensen, Real-time UV imaging of nicotine release from transdermal patch, *Pharmaceut. Res.* 27 (12) (2010) 2614–2623.
- [29] J. Østergaard, J.X. Wu, K. Naelapää, J.P. Boetker, H. Jensen, J. Rantanen, Simultaneous UV imaging and Raman spectroscopy for the measurement of solvent-mediated phase transformations during dissolution testing, *J. Pharmaceut. Sci.* 103 (4) (2014) 1149–1156.
- [30] J.P. Boetker, J. Rantanen, T. Rades, A. Müllertz, J. Østergaard, H. Jensen, A new approach to dissolution testing by UV imaging and finite element simulations, *Pharmaceut. Res.* 30 (5) (2013) 1328–1337.
- [31] J. Østergaard, UV imaging in pharmaceutical analysis, *J. Pharmaceut. Biomed. Anal.* 147 (2018) 140–148.
- [32] A. Ward, K. Walton, S. Stoycheva, M. Wallis, A. Adebisi, E. Nep, N.C. Ngwuluka, S. Shaboun, A.M. Smith, B.R. Conway, K. Asare-Addo, The use of visible and UV dissolution imaging for the assessment of propranolol hydrochloride in liquidoid compacts of Sesamum radiatum gum, *J. Drug Deliv. Sci. Technol.* (2020) 101511.
- [33] Y. Sun, A. Chapman, S.W. Larsen, H. Jensen, N.J. Petersen, D.M. Goodall, J. Østergaard, UV–vis imaging of piroxicam supersaturation, precipitation, and dissolution in a flow-through setup, *Anal. Chem.* 90 (11) (2018) 6413–6418.
- [34] K. Asare-Addo, K. Walton, A. Ward, A.-M. Totea, S. Taheri, M. Alshafiee, N. Mawla, A. Bondi, W. Evans, A. Adebisi, B.R. Conway, P. Timmins, Direct imaging of the dissolution of salt forms of a carboxylic acid drug, *Int. J. Pharm.* 551 (1–2) (2018) 290–299.
- [35] K. Asare-Addo, M. Alshafiee, K. Walton, A. Ward, A.-M. Totea, S. Taheri, N. Mawla, A.O. Adebisi, S. Elawad, C. Diza, P. Timmins, B.R. Conway, Effect of preparation method on the surface properties and UV imaging of indomethacin solid dispersions, *Eur. J. Pharm. Biopharm.* 137 (2019) 148–163.
- [36] F. Alqahtani, P. Belton, A. Ward, K. Asare-Addo, S. Qi, An investigation into the use of low quantities of functional additives to control drug release from hot melt extruded solid dispersions for poorly soluble drug delivery, *Int. J. Pharm.* (2020), 2020;579 119172.
- [37] A. Ward, K. Walton, N. Mawla, W. Kaiyaly, L. Liu, P. Timmins, B.R. Conway, K. Asare-Addo, Development of a novel method utilising dissolution imaging for the measurement of swelling behaviour in hydrophilic matrices, *Int. J. Pharm.* X 1 (2019) 100013.
- [38] P. Madelung, P. Bertelsen, J. Jacobsen, A. Müllertz, J. Østergaard, Dissolution enhancement of griseofulvin from griseofulvin-sodium dodecyl sulfate discs investigated by UV imaging, *J. Drug Deliv. Sci. Technol.* 39 (2017) 516–522.
- [39] T.N. Hiew, M.I. Alaudin, S.M. Chua, P.W. Heng, A study of the impact of excipient shielding on initial drug release using UV imaging, *Int. J. Pharm.* 553 (1–2) (2018 Dec 20) 229–237.
- [40] A. Nokhodchi, A. Homayouni, R. Araya, W. Kaiyaly, W. Obeidat, K. Asare-Addo, Crystal engineering of ibuprofen using starch derivatives in crystallization medium to produce promising ibuprofen with improved pharmaceutical performance, *RSC Adv.* 5 (57) (2015) 46119–46131.
- [41] D.K. Bučar, J.A. Elliott, M.D. Eddleston, J.K. Cockcroft, W. Jones, Sonocrystallization yields monoclinic paracetamol with significantly improved compaction behavior, *Angew. Chem. Int. Ed.* 54 (1) (2015) 249–253.
- [42] P. Di Martino, A.M. Guyot-Hermann, P. Conflant, M. Drache, J.C. Guyot, A new pure paracetamol for direct compression: the orthorhombic form, *Int. J. Pharm.* 128 (1) (1996) 1–8.
- [43] K. Walton, L. Fleming, M. Goodhand, R. Racasan, W. Zeng, High fidelity replication of surface texture and geometric form of a high aspect ratio aerodynamic test component, *Surf. Topogr. Metrol. Prop.* 4 (2) (2016) 25003.
- [44] K. Walton, L. Blunt, L. Fleming, The topographic development and areal parametric characterization of a stratified surface polished by mass finishing, *Surf. Topogr. Metrol. Prop.* 3 (3) (2015) 35003.
- [45] K. Walton, L. Blunt, L. Fleming, M. Goodhand, H. Lung, Areal parametric characterisation of ex-service compressor blade leading edges, *Wear* 321 (2014) 79–86.
- [46] Convention Usp, First Supplement to USP 42-NF37, United States Pharmacopeial Convention., Rockville, Maryland, 2019.
- [47] Taylor Hobson UoH, Surfstand, Huddersfield, 2013.
- [48] F. Helmlí, Focus Variation Instruments, Springer Berlin Heidelberg, Berlin, Heidelberg, 2011, pp. 131–166.
- [49] C. Al-Karawi, T. Kaiser, C.S. Leopold, A novel technique for the visualization of tablet punch surfaces: characterization of surface modification, wear and sticking, *Int. J. Pharm.* 530 (1–2) (2017 Sep 15) 440–454.
- [50] P.R. Laity, K. Asare-Addo, F. Sweeney, E. Šupuk, B.R. Conway, Using small-angle X-ray scattering to investigate the compaction behaviour of a granulated clay, *Appl. Clay Sci.* 108 (2015) 149–164.
- [51] A.A. Rose, W. Kaiyaly, Improved tableting behavior of paracetamol in the presence of polyvinylpyrrolidone additive: effect of mixing conditions, *Particuology* 43 (2019) 9–18.
- [52] M. Khanmohammadi, A.B. Garmarudi, N. Moazzen, K. Ghasemi, Qualitative discrimination between paracetamol tablets made by near infrared spectroscopy and chemometrics with regard to polymorphism, *J. Struct. Chem.* 51 (4) (2010) 663–669.